Cloud effective transmittance at two sites of the Atacama Desert, Chile

Eduardo Luccini,[1,2] Miguel Rivas,[3] Elisa Rojas,[3] and Pablo Canziani[4,5]

Received 6 March 2011; revised 21 July 2011; accepted 23 July 2011; published 22 October 2011.

[1] Broadband overcast cloud effective transmittance was determined at Arica (18.47°S, 70.31°W, 20 m above sea level (asl)) and Poconchile (18.45°S, 70.07°W, 560 m asl), Atacama Desert, northern Chile, from 10 min averaged pyranometer measurements of total solar irradiance (ToSI) and ultraviolet solar irradiance (UVSI) during the period 2002–2005. The predominant cloud type is marine stratocumulus, characteristic of the southeastern Pacific tropical environment. The region's very regular climate conditions, characterized by overcast mornings and cloudless afternoons, allow the application of an empirical method to determine the expected clear-sky irradiance during cloudy mornings. The cloud effective transmittance (CET) is determined as the ratio of the measured cloudy-sky irradiance over the expected clear-sky irradiance. $CET_{To} = 0.26$ (0.31) for ToSI and $CET_{UV} = 0.37$ (0.43) for UVSI characterize overcast cloudiness at Arica (Poconchile). One-dimensional radiative transfer model calculations in both ToSI and UVSI ranges are also used. The measured and modeled relationships between CET_{To} and CET_{UV} closely agree. New insights are given to explain the sparsely populated data around CET = 0.8 observed also by other similar studies.

Citation: Luccini, E., M. Rivas, E. Rojas, and P. Canziani (2011), Cloud effective transmittance at two sites of the Atacama Desert, Chile, *J. Geophys. Res.*, *116*, D20205, doi:10.1029/2011JD015905.

1. Introduction

[2] Clouds play a fundamental role on the Earth's environment. Knowing their microphysical and optical properties is crucial to understand and quantify their radiative effects on climate. The cloud effective transmittance (CET) is defined as the ratio of the surface irradiance under cloudy conditions to the expected surface irradiance that would be registered for a cloudless sky. It is a commonly cited cloud optical parameter as it represents the actual attenuation of solar irradiance by the cloud cover, with important biological and photochemical consequences. Among other applications, it is used in different algorithms to estimate more detailed cloud optical parameters from ground-based measurements, like cloud optical depth (COD) and cloud droplet equivalent radius (r_e) [e.g., *Leontieva and Stamnes*, 1996; *Boers et al.*, 2000].

[3] There are few regions in the world where climate conditions are so regular and stable as they are in Atacama, the driest and oldest extant desert on Earth [*Hartley et al.*, 2005] (http://www.unep.org/Geo/gdoutlook/), along the South American Pacific coast. Extreme dryness is maintained for several reasons: the Andes Mountains on South America's west act as a barrier to the incursion of wet air from the Amazonian circulation, the South Pacific Anticyclone generates a regular thermal inversion layer along the coast, and the cold Humboldt marine current of the eastern Pacific strongly limits seawater evaporation [*Cereceda et al.*, 2002]. Even small changes in the climate of the Atacama Desert may be considered as insights of evidence of the Global Climate Change, currently under way (http://www.ipcc.ch/ipccreports/ar4-syr.htm).

[4] The South Pacific Ocean contains one of the more persistent stratocumulus systems in the world. Moreover this is the area where El Niño/La Niña phenomena develop, which have influence over the whole planet. Clouds over the continent are also very important in this region. In some areas, they determine the possibility of sustaining vegetation and they provide a local source of pure water from the local fog known as "camanchaca" [*Schemenauer et al.*, 1988]. In turn, they constitute an attenuation agent of solar UV radiation in this tropical area where clear-sky UV radiation levels are extreme (UV Index ≥ 11) during most of the year [*Rivas et al.*, 2000], motivating important public health campaigns [*Rivas et al.*, 2008]. *Cereceda et al.* [2008a] have extensively studied the climate of the region, distinguishing two zones from the coast inland to the east, whose characteristics are linked to the pres-

[1]Grupo de Energía Solar, Instituto de Física de Rosario, Consejo Nacional de Investigaciones Científicas y Técnicas, Rosario, Argentina.
[2]Facultad de Química e Ingeniería, Pontificia Universidad Católica Argentina, Rosario, Argentina.
[3]Laboratorio de Radiación Solar Ultravioleta, Departamento de Física, Facultad de Ciencias, Universidad de Tarapacá, Arica, Chile.
[4]Consejo Nacional de Investigaciones Científicas y Técnicas, Buenos Aires, Argentina.
[5]Equipo Interdisciplinario Para el Estudio de Procesos Atmosféricos en el Cambio Global, Pontificia Universidad Católica Argentina, Buenos Aires, Argentina.

0148-0227/11/2011JD015905

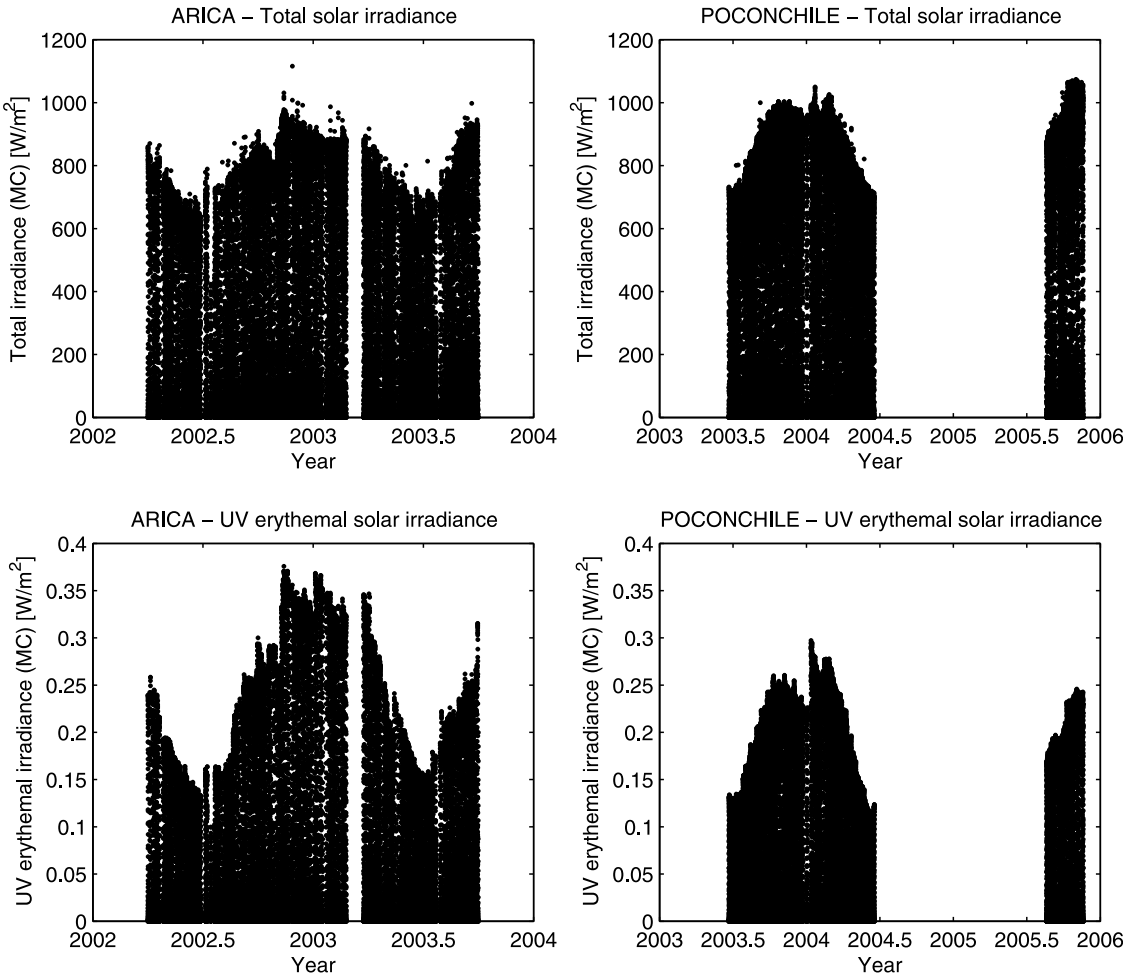

Figure 1. Ten minute averaged measurements of solar irradiance at (left) Arica and (right) Poconchile as a function of the date for days with cloudless afternoons, specifically selected to determine the cloud effective transmittance. (top) Total solar irradiance. (bottom) UV solar irradiance. Data respond to the manufacturer calibration (MC) of the instruments.

ence of stratocumulus clouds: a "coastal desert with abundant cloudiness" from sea level up to an altitude of about 650 m, and a "desert with abundant fog" from about 650 m up to 1200 m.

[5] In this work, a study of CET is made from pyranometer measurements at two locations in the northern Chile's Atacama Desert: the coastal city of Arica, within the climate defined as "coastal desert with abundant cloudiness," and the inland locality of Poconchile, at an altitude where fog related to the same kind of cloudiness begins to be relevant. The region's regular climate provides a reliable empirical way to determine the expected clear-sky irradiance for each measurement under cloudy sky, as mornings remain generally with overcast sky and cloudiness quickly dissipates toward noon, giving cloudless afternoons. The determined CET is independent of the absolute calibration of the instruments. Our analysis uses measurements and 1-D model irradiance calculations in both ToSI (300–3000 nm) and UVSI (280–400 nm erythemally weighted) broadband ranges.

2. Measurements

[6] Solar irradiance on a horizontal plane was measured at the tropical Pacific coastal city of Arica (18.47°S, 70.31°W, 20 m above sea level (asl)) and at Poconchile site (18.45°S, 70.07°W, 560 m asl), about 30 km inland from the coast, both in the north part of the Atacama Desert, Chile. Measurements were made in the period March 2002–September 2003 at Arica, and during the periods June 2003–June 2004 and August–November 2005 at Poconchile. Figure 1 shows the whole selected measurements database as a function of the date.

[7] ToSI (300–3000 nm) was measured with pyranometers Solar Light 1141, S/N 5019 at Arica and S/N 5020 at Poconchile. UV erythemal irradiance, following the action spectrum of typical human skin [*McKinlay and Diffey*, 1987], was measured with UV biometers Solar Light 501A, S/N 4425 at Arica and S/N 4423 at Poconchile. Data were recorded as 10 min averages with Campbell CR10X data loggers, S/N X21235 at Arica and S/N X21236 at Poconchile. The solar zenith angle (SZA) for each measurement was determined at the center of each 10 min interval. The denominator of CET corresponds mostly to clear-sky conditions and is sensitive to both the cosine response and the thermal offset due to infrared cooling of the instruments, whereas the numerator of CET corresponds to cloudy-sky

Figure 2. Panoramic view at Arica of the morning cloudiness typical behavior over the Atacama Desert. (top left) 17 March 2009, 0840 LT, overcast sky. (bottom left) 17 March 2009, 1149 LT, cloudiness begins to break out. (top right) 17 March 2009, 1240 LT, cloudiness vanishes. (bottom right) Panoramic aerial view of the typical homogeneous layer cloudiness top, 24 March 2009, 0730 LT.

conditions and is less affected by these effects. Manufacturer-estimated precision by cosine response is within 2% for Solar Light 1141 and 5% for Solar Light 501A for direct-beam incidence at angles less than 70°. We have not the complementary instruments required to accurately determine the offset due to infrared cooling for total shortwave thermopile sensors [*Dutton et al.*, 2001]. However, the dark-signal night offset of all instruments was analyzed. 62% (93%) of over 20,000 Solar Light 1141 nighttime raw data were equal to zero at Arica (Poconchile), with a maximum of 2.4 (7.2) W/m^2 and no negative values, respectively. The absence of negative values may be due to the large percentage of nights under overcast sky conditions, cloudiness that remains during the morning. UV biometers are not affected by thermal offset under clear skies, and nighttime raw data of Solar Light 501A were always zero. Then, in practice no dark-signal offset correction was implemented. The irradiance offset due to thermal effect is not dependent on the SZA. Then, when applied to the relative parameter CET, both cosine response and thermal effects act principally in the range of SZA > 80° which for this reason is excluded from the analysis. In turn, given that both cosine response and thermal effects cause slightly smaller values on the denominator of CET, we assume that for SZA < 80° our reported CET are slightly overestimated. Manufacturer-provided calibrations of all instruments were used. It is a known fact that, particularly in the UV range, the manufacturer's calibration is not precise enough for scientific analysis based on absolute values [e.g., *Leszczynski et al.*, 1998]. This is clearly seen in Figure 1 where seasonal maximum UV absolute values at Arica, at sea level, are markedly larger than those from the close higher-altitude station of Poconchile. However, as will be described in section 3, this is irrelevant for the present work since CET is a relative parameter obtained from measurements by the same instrument, and therefore it is independent of the instrument's absolute calibration.

3. Determination of the Cloud Effective Transmittance

[8] To obtain the CET, each irradiance measurement under a cloudy condition must have their expected irradiance that would be registered for a cloudless sky. For this purpose, we make use of the notable climatic regularity of the region. As mentioned, along the coastal region of the Atacama Desert the overcast sky is generally present during the morning hours, then toward noon the cloudiness quickly breaks down and vanishes, resulting in cloudless afternoons. Figure 2 documents photographically an example of this typical cloudiness behavior, on different moments of day 17 March 2009, together with an aerial view of the homogeneous cloud top, on day 24 March 2009. The first step was to select those days with mostly cloudless afternoons from the observations database. At Arica (Poconchile),

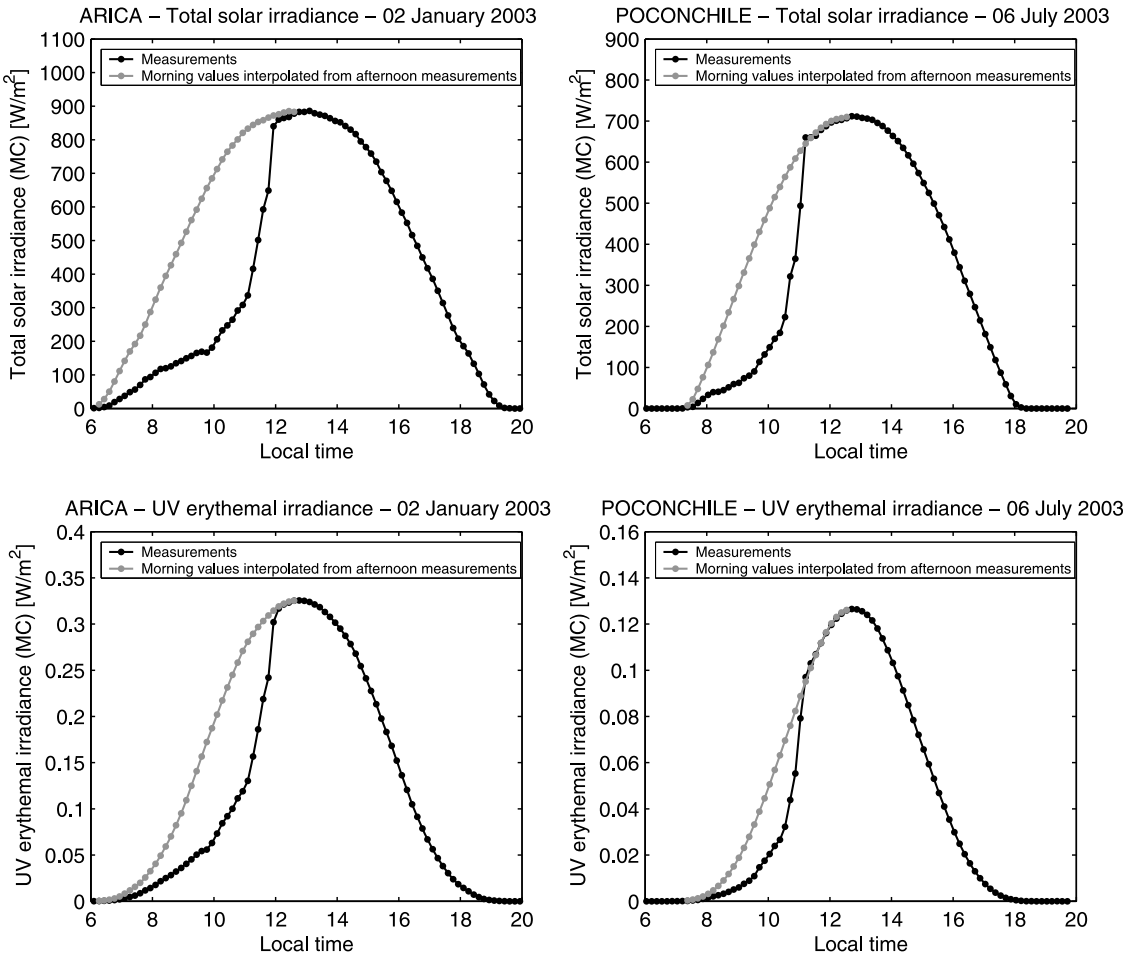

Figure 3. Example of the analysis method from 10 min averaged measurements made on (left) 2 January 2003 at Arica and (right) 6 July 2003 at Poconchile. The expected clear-sky irradiance values during the morning (shaded line and dots) are interpolated from the afternoon values at the solar zenith angle (SZA) of the morning measurements. Data respond to the MC of the instruments. (top) Total solar irradiance. (bottom) UV solar irradiance. The ratio of cloudy over expected clear-sky irradiance values is the cloud effective transmittance (CET).

365 (358) days from the whole database of 517 (456) days, i.e., 70% (78%) of days were found to meet this criterion; they are shown in Figure 1. Given that every clear-sky irradiance plot mirrors about solar noon, the expected clear-sky irradiance values during the morning were interpolated from the afternoon values at the SZA of the morning measurements. Figure 3 shows examples of the method applied, for days 2 January 2003 at Arica and 6 July 2003 at Poconchile.

[9] The method has several advantages. The expected clear-sky irradiance is directly obtained and no indirect estimate is necessary, such as model calculations of the absolute irradiance. No absolute calibration of the instruments is required, as CET is a relative parameter obtained from measurements made with the same instrument. Furthermore, given that it is based on measurements made within the same day, no matter what the specific values of related parameters like ozone and aerosols were, as they are usually considered constant during each day for this type of application.

[10] This method was applied to each selected day, having a predominantly cloudless afternoon. Figure 4 shows the CET determined from each irradiance measurement during the morning, when the sky generally presents an overcast sky, for the ToSI and UVSI at Arica and Poconchile. As mentioned, data for SZA > 80° were excluded since the uncertainties both in measurements and in 1-D model calculations substantially increase [*Barker et al.*, 1998; *Dong et al.*, 1998; *Barnard and Long*, 2004]. Cloudiness is present from before dawn through late morning, and CET has its lower values <1 for large SZA. As the morning advances and SZA decreases, cloudiness generally vanishes and points tend to group in values close to 1. As can be noted, the effects of clouds are stronger on the ToSI than on the UVSI including both the attenuation and the enhancement of irradiance, in agreement with the wide evidence that clouds more intensely affect the ToSI than the UVSI in all-sky conditions. This is due to the fact that the relative contribution of the direct component with respect to the diffuse one at the surface is always larger in ToSI than in UVSI [e.g., *Cede et al.*, 2002a;

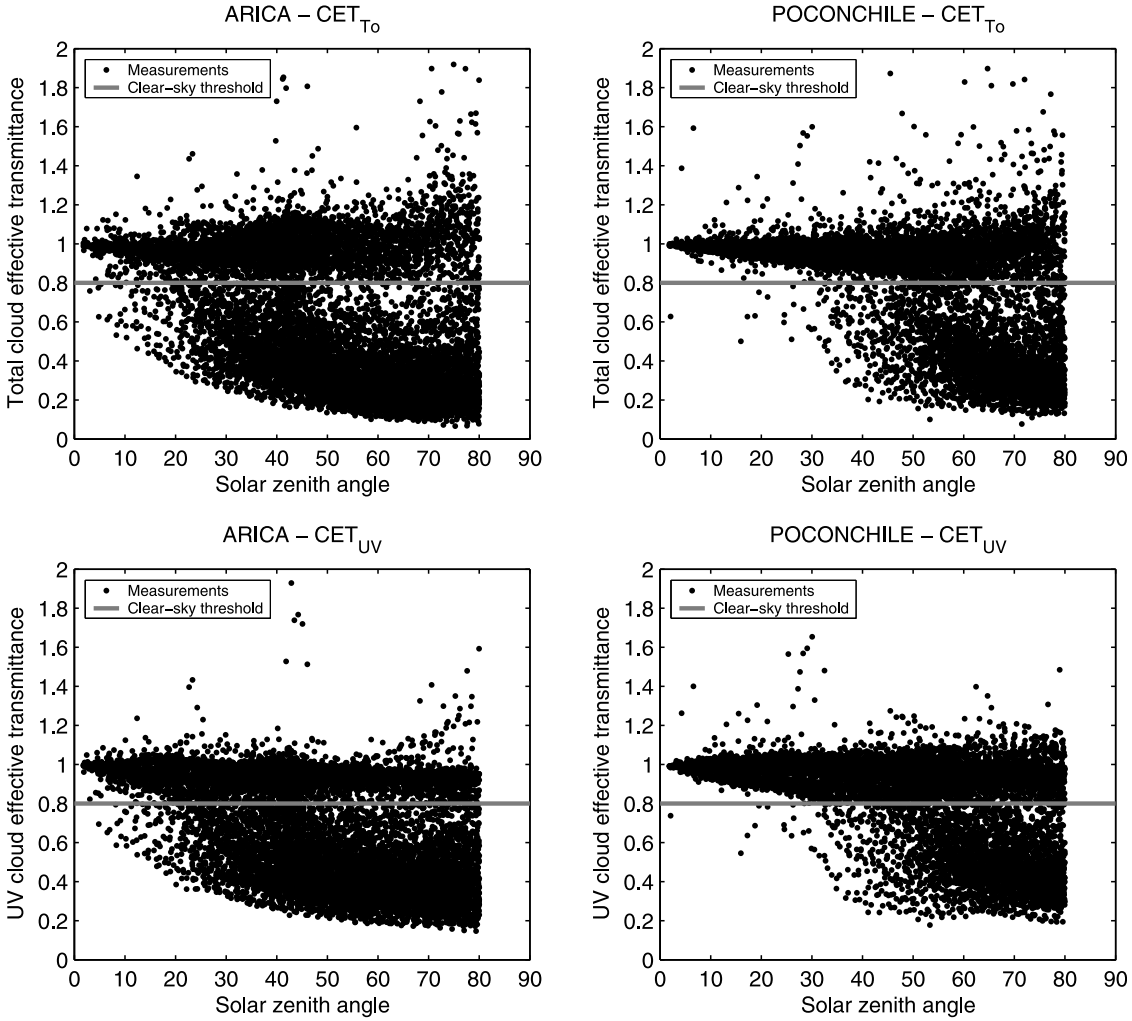

Figure 4. CET determined from 10 min averaged morning measurements at (left) Arica and (right) Poconchile in the (top) total range and in the (bottom) UV range as a function of the solar zenith angle. An empirical threshold of CET = 0.80 (shaded line) is established so that only points with CET < 0.80 are considered as corresponding to cloudy conditions. Data for SZA > 80° were excluded due to their larger uncertainty.

Calbó et al., 2005]. For the same reason, CET_{To} is much more sensitive than CET_{UV} to variations in the SZA at constant COD, as will be noted in section 4. Four data clusters can be observed in Figure 4, as follows.

[11] 1. The few points with CET > 1.1 may be explained in part by the surface solar irradiance enhancing by reflection off of the sides of clouds [e.g., *Mims and Frederick*, 1994], even though broken stratocumulus characteristic of this region do not reach the needed vertical development to magnify this effect. More probably, given the employed method to determine the expected clear-sky solar irradiance, they may be caused by occasional moments when some isolated cloud obscured the direct sun during the afternoon. This is not a problem to apply the method given that only these isolated points were affected, and the afternoon downwelling solar irradiance for close points under very scattered clouds with exposed direct sun is basically the same that under a clear sky.

[12] 2. Given that the region is characterized by an important aerosol content, eventual diurnal aerosol variations cause the spread of values around CET = 1, basically between CET ~ 0.9 and CET ~ 1.1, which does not significantly influence the cloud analysis. This agrees with the concept of thick-aerosol-related broadening of the clear-sky states by *Charlson et al.* [2007].

[13] 3. The sparsely populated area of measured transmittances around CET = 0.80, which is wider and more evident in ToSI than in UVSI as expected from the mentioned effects of clouds. It is similar to that which *Fitzpatrick and Warren* [2005] named the "Köhler gap," under the argument that it may be due to the threshold nature of the aerosol-to-cloud-droplet transition evidenced in low-aerosol-content regions. In contrast, *Charlson et al.* [2007] concluded that the transition states between cloudy-sky and clear-sky are in general a smooth continuous, due to the significant presence of non-visible small-COD wispy clouds. In our case, we find two complementary explanations from the measurements and from the model calculations: the regularity of the analyzed meteorological phenomenon allows us to infer that, for SZA < ~50°, this less populated data zone represents the quick cloud breaking in the transition from the overcast-sky

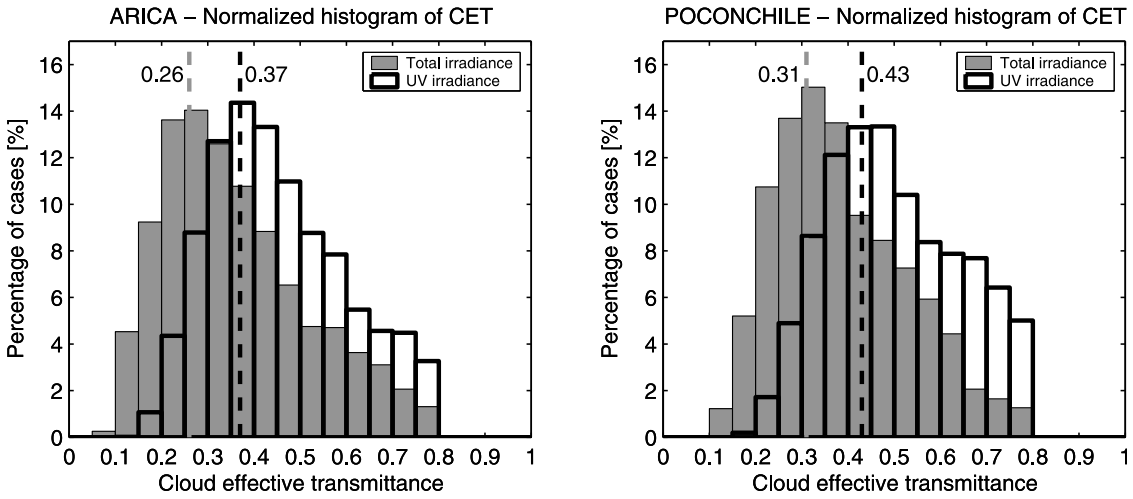

Figure 5. Normalized histograms of the measured CETs for the cloudy cases of Figure 4 (CET < 0.80) in the total range (shaded bars) and in the UV range (solid contour bars) at (left) Arica and (right) Poconchile. Dashed lines, taken from a smoothed curve, denote the maximum concentration of points. They characterize the typical CET for homogeneous overcast-sky conditions in both the total (shaded) and UV (solid) ranges.

to the clear-sky states each morning, lasting around 30–50 min, i.e., only 3–5 points at 10 min averages in Figure 4 (see also the example of Figure 2). For SZA > ~50°, the sky is basically under one of two opposite conditions: cloudless or homogeneous overcast cloudiness of significant COD, and as a consequence few points fall in the range of ~0.5 < CET < 0.8. Additionally model calculations, which will be detailed in section 4, show that under overcast sky the CET decreases progressively when the SZA increases at constant COD. This is more evident for small COD (<10), causing an area of sparsely populated data around CET = 0.8 for SZA > ~50°.

[14] 4. The area of Figure 4 with maximum concentration of points below CET = 0.8 represents more precisely the homogeneous overcast sky conditions.

[15] From the previous analysis, CET = 0.80 may be established as an empirical threshold to distinguish the clear-sky from the cloudy-sky data at both sites and for both wavelength ranges, such as only points with CET < 0.80 are considered cloudy events. Figure 5 shows the histograms of the measured CET values for cloudy cases (CET < 0.8) from Figure 4. As expected, distributions are asymmetric, since they cover the sparse data area close to CET = 0.8 and the larger data concentration of homogeneous overcast sky cases for smaller values of CET. Points around the maximum of the histograms are in fact those that actually characterize the homogeneous overcast sky conditions, corresponding to CET_{To} = 0.26 (0.31) for ToSI and CET_{UV} = 0.37 (0.43) for UVSI at Arica (Poconchile). They are also emphasized in Figure 5. This implies that overcast cloudiness attenuates about 70% of the ToSI and about 60% of the UVSI with respect to the clear-sky values in the region. If all-cloudiness conditions are to be considered, mean values are CET_{To} = 0.36 (0.39) and CET_{UV} = 0.45 (0.50) at Arica (Poconchile), implying that morning cloudiness attenuates in general about 60%–65% of the ToSI and about 50%–55% of the UVSI on average with respect to the clear-sky values. It is interesting to note that the observed absolute minimum are CET_{To} ~ 0.1 and CET_{UV} ~ 0.2 at both sites. They put a limit to the maximum COD registered in the region.

4. Model Calculations

[16] Model calculations were made to establish a theoretical reference of CET_{To}, CET_{UV} and their relation. As mentioned by *Loeb and Coakley* [1998] overcast marine stratus, the kind of cloudiness here considered and depicted in Figure 2, constitute the closest condition to the ideal homogeneous plane-parallel water cloud layer, suitable for application of plane-parallel 1-D radiative transfer models. A single cloud layer is considered in the model. In turn, measurements include the effect of any other real clouds above the observed cloud layer, and/or fog. Nevertheless, *Ayers et al.* [2001, 2002] showed that the fraction of ice clouds above the stratocumulus deck is typically very small in this region, less than 15%, so that the modeled single cloud layer represents appropriately the measurement conditions for most of cases.

[17] Radiative transfer calculations of instantaneous ToSI and UVSI irradiances for the SZA range 0°–90° were made with the plane-parallel 1-D Fu-Liou online code (Diurnal Simulation page, http://snowdog.larc.nasa.gov/cgi-bin/rose/flp200503/sun/flsun.cgi) [*Fu and Liou*, 1992, 1993; *Rose and Charlock*, 2002], four-stream algorithm, with a standard tropical vertical atmospheric structure. UV Index calculations with the Fu-Liou model (corresponding to UV erythemal irradiance) showed appropriate CET values for each COD, but its behavior as a function of the SZA is reasonable only within the range 0° ≤ SZA < 30°. Then, UVSI was calculated with the Fu-Liou model for the UVA range (320–400 nm) given that it corresponds to an atmospheric absorption window and, under the assumption that cloud optical properties are spectrally flat in the UV, the ratio of UVA irradiances will be very similar to the ratio of UV erythemal irradiances. Additionally, Fu-Liou UVA calculations were compared against the UV erythemal irradiance obtained with a Discrete

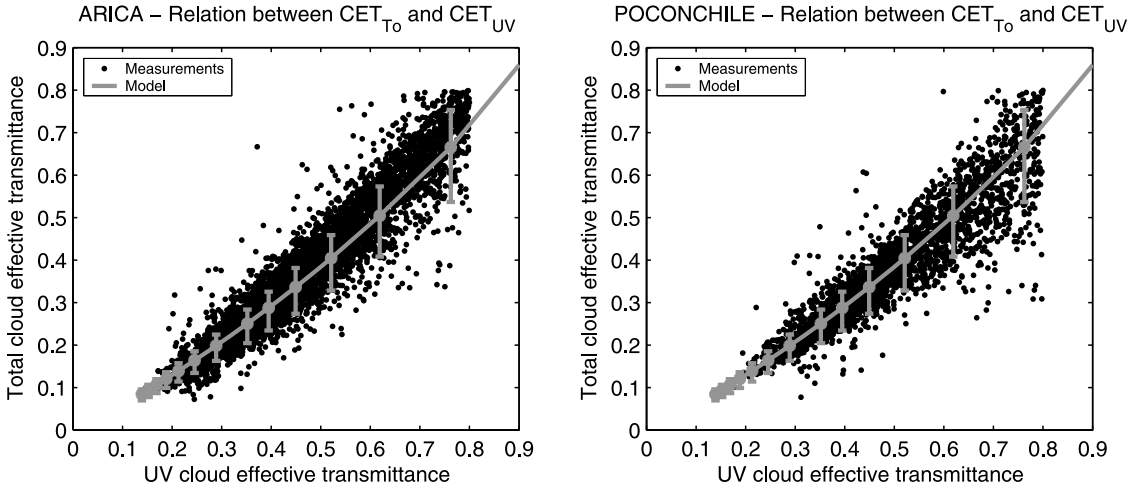

Figure 6. Relation between the cloud effective transmittance in the total range (CET_{To}) and the cloud effective transmittance in the UV range (CET_{UV}) at (left) Arica and (right) Poconchile. Solid circles are from simultaneously measured 10 min averages. The shaded line is the average modeled relation from calculations with the Fu-Liou code. Bars at each modeled point denote the SZA variation; the maximum CET_{To} values are obtained for SZA = 0°, and the minimum ones are obtained for SZA = 80°.

Ordinates (DISORT) algorithm with pseudo-spherical correction for the direct irradiance [see, e.g., *Cede et al.*, 2002b; *Luccini et al.*, 2006]. CET absolute differences of the Fu-Liou UVA with respect to the DISORT UV erythemal irradiance were small, of 0.01, 0, and –0.04 for COD = 5, 20, and 50 for 0° ≤ SZA < 80°, respectively. In order to avoid discrepancies that may appear by the use of different radiative transfer codes, we used only calculations with the Fu-Liou model.

[18] From the analysis by *Cereceda et al.* [2008b] and the advice from the meteorologists of the Chilean National Weather Service station at the airport of Arica, a homogeneous infinite plane-parallel cloud layer of 400 m thickness with cloud base at 900 m asl and cloud top at 1300 m asl was considered representative of the local overcast stratocumulus-type cloudiness. Satellite-derived surface albedo for ToSI over this coastal desert land shows values predominantly around 0.20 [*Minnis and Harrison*, 1984; *Tsvetsinskaya et al.*, 2006]. The ocean broadband ToSI albedo is typically between 0.07 and 0.09 [*Fitzpatrick et al.*, 2004; *Li and Garand*, 1994]. In turn, satellite-derived UVSI surface albedo is slightly smaller than the corresponding broadband ToSI albedo in this region for both the coastal desert (0.08–0.12) and ocean (0.03–0.06) [*Herman and Celarier*, 1997]. Given that the surface albedo in a radius of several kilometers influences the irradiance at a given place (over 40 km in the UV range [*Degünther et al.*, 1998; *Degünther and Meerkötter*, 1998]), a broadband surface albedo of 0.10 was considered appropriate in both the ToSI and UVSI, which may be considered as a geographical average over this coastal region. Nevertheless, given that CET consists in the ratio of downwelling solar irradiances, differences in the calculated solar irradiances due to a slightly different actual average surface albedo cause negligible changes on CET. A 270 DU total vertical ozone column was used, it being a typical value over this tropical region where ozone values have a small seasonal fluctuation [e.g., *Rivas et al.*, 2000]. AERONET data from the instrument installed at Arica show that the presence of aerosols is important in the region, and that the particles have a relatively small size [*Otero et al.*, 2006]. A 0.3 average aerosol optical depth (at 440 nm) with an Angstrom exponent of 1.2 was used for the calculations in both ToSI and UVSI. From retrievals of the Moderate Resolution Imaging Spectroradiometer (MODIS) satellite instrument [*Wood et al.*, 2006], a relatively small value of $r_e = 8$ μm was used which seems to be directly related to the sulfur emissions from the nearby big copper smelters transported by the region's predominant winds from the S-SE [*Huneeus et al.*, 2006; *Wood et al.*, 2006].

[19] Broadband downwelling irradiance calculations at the surface for overcast sky were made for COD equal to 5, 10, 15, 20, 25, 30, 40, 50, 60, 70, 80, 90, and 100, and for 0°–90° SZA range. COD was set to 0 for the clear-sky case. Then, CET was determined for each COD value, as the ratio of the cloudy case over the clear-sky case as a function of SZA. The same modeled CET were used for Arica and Poconchile, as the different altitude of both locations produces negligible differences in the ratio of calculated irradiances.

[20] Model calculations reaffirm the fact that the SZA dependence at constant COD is much more pronounced in CET_{To} than in CET_{UV}. For this reason, CET_{To} is plotted as a function of CET_{UV} in Figure 6 as obtained from simultaneous ToSI and UVSI 10 min averaged measurements and also as calculated from the Fu-Liou model. To establish the average modeled curve, it is assumed as a first approximation that COD_{To} and COD_{UV} have the same value at each point. Bars in the average modeled curve represent the variability with the SZA, where calculations show that the maximum CET values correspond to SZA = 0° and the minimum ones to SZA = 80°. This is because CET decreases progressively when SZA increases at constant COD, due to a larger proportion of the incoming direct solar irradiance scattered back upward by reflection from the homogeneous cloud top. The sparsely populated area of measured data in Figure 4, mentioned in section 3, is observed in Figure 6 below the average modeled

curve between $CET_{UV} \sim 0.5$ and $CET_{UV} = 0.8$. Measured and modeled values show a very good agreement at both sites. As expected from the mentioned cloud effects on ToSI and UVSI for irradiance attenuation cases, the average CET_{To} is always smaller than the average CET_{UV} at both sites.

5. Conclusions

[21] The cloud effective transmittance for overcast coastal stratocumulus were determined at Arica and Poconchile, representative sites of the Atacama Desert in the north of Chile, the driest region in the world, using 10 min averaged solar irradiance broadband pyranometer measurements in both the total and UV ranges. The regional climate regularity, with typical cloudy mornings and cloudless afternoons, allowed for the application of an empirical method to determine the expected clear-sky irradiance during the morning using the afternoon's measurements of each day.

[22] Characteristic cloud effective transmittance for overcast-sky conditions is about 0.30 in ToSI and 0.40 in UVSI, while for all-cloudiness conditions it is around 0.35–0.40 in ToSI and 0.45–0.50 for UVSI. This implies that overcast cloudiness attenuates about 70% of the ToSI and about 60% of the UVSI with respect to the clear-sky values in the region, and that morning cloudiness attenuates in general about 60%–65% of the ToSI and about 50%–55% of the UVSI on average with respect to the clear-sky values. Thus the attenuation of solar radiation by this regularly present cloudiness may be considered significant, particularly in the UVSI range in a region where extreme UV Index values (11+) are common during most of the year. Fog is also often present at intermediate altitudes like that of Poconchile, associated to occasional lower-base events of the same kind of cloudiness, and its effect is included in the present results. Databases are not extensive enough to analyze the CET's seasonal behavior.

[23] The important aerosol content of this region, and its eventual daily variation, causes the spread of values around CET = 1, between CET ~ 0.9 and CET ~ 1.1, evidencing the concept of thick-aerosol-related broadening of the clear-sky states.

[24] New insights have been provided about the sparsity of CET data as a function of the SZA around CET = 0.8, referred to by other authors but still without a concrete explanation. At least for the regular climate conditions characterizing the Atacama Desert, we have found two main reasons that could explain it: the quick breaking of the overcast cloudiness in the transition toward a clear sky, added to the progressive decrease of CET at constant COD for increasing SZA due to the relative increase in the fraction of the incoming direct solar irradiance being scattered back upward by reflection in the homogeneous cloudiness top, more evident for small values of COD (<10).

[25] The reliability of the CET values here obtained from measurements through a method that is independent of the absolute calibration of the instruments, and the agreement between measurements and 1-D model calculations, encourage their joint use to estimate from irradiance ground measurements more detailed cloud parameters like the cloud optical depth. Many international efforts are currently being devoted to study the cloud properties in the South Pacific Ocean, and every contribution from the adjacent continental zone is an important complement. The high content of natural aerosols, the anthropogenic sulfur emissions from the copper smelters in the region, and the occasional natural volcanic emissions transported by the zonal winds add particularities to the local environment.

[26] Thus, the results here obtained must be taken as a preliminary approach to promote new and more detailed investigations on cloud properties over the coastal Pacific region of South America. The recent inclusion of new equipment may allow more sophisticated studies in the future. Long-term measurements of atmospheric parameters at such climatically stable regions are very important to enhance the capacity for detecting and monitoring global climate change processes.

[27] **Acknowledgments.** This research was supported by Proyecto de Investigación Mayor code 4721-2011, Universidad de Tarapacá, Arica, Chile, and the Consejo Nacional de Investigaciones Científicas y Técnicas (CONICET), Agencia Nacional de Promoción Científica y Tecnológica (ANPCyT), Universidad Nacional de Rosario and Pontificia Universidad Católica of Argentina. The authors acknowledge the interesting comments by the anonymous reviewers that contributed to the improvement of this work.

References

Ayers, J. K., P. Minnis, D. F. Young, W. L. Smith Jr., and L. Nguyen (2001), Development of a climatology of cloud properties over the southeastern Pacific for PACS, paper presented at 11th Conference on Satellite Meteorology and Oceanography, Am. Meterol. Soc., Madison, Wis., 15–18 Oct.

Ayers, J. K., P. Minnis, P. W. Heck, A. D. Rapp, D. F. Young, W. L. Smith Jr., and L. Nguyen (2002), A one-year climatology of cloud properties derived from GOES-8 over the southeastern Pacific for PACS, paper presented at the 11th Conference on Cloud Physics, Am. Meteorol. Soc., Ogden, Utah.

Barker, H. W., T. J. Curtis, E. Leontieva, and K. Stamnes (1998), Optical depth of overcast cloud across Canada: Estimates based on surface pyranometer and satellite measurements, *J. Clim.*, *11*, 2980–2994, doi:10.1175/1520-0442(1998)011<2980:ODOOCA>2.0.CO;2.

Barnard, J. C., and C. N. Long (2004), A simple empirical equation to calculate cloud optical thickness using shortwave broadband measurements, *J. Appl. Meteorol.*, *43*, 1057–1066, doi:10.1175/1520-0450(2004)043<1057:ASEETC>2.0.CO;2.

Boers, R., A. Van Lammeren, and A. Feijt (2000), Accuracy of cloud optical depth retrievals from ground-based pyranometers, *J. Atmos. Oceanic Technol.*, *17*, 916–927, doi:10.1175/1520-0426(2000)017<0916:AOCODR>2.0.CO;2.

Calbó, J., D. Pagès, and J. González (2005), Empirical studies of cloud effects on UV radiation: A review, *Rev. Geophys.*, *43*, RG2002, doi:10.1029/2004RG000155.

Cede, A., E. Luccini, L. Nuñez, R. Piacentini, and M. Blumthaler (2002a), Effects of clouds on erythemal and total irradiance as derived from data of the Argentine Network, *Geophys. Res. Lett.*, *29*(24), 2223, doi:10.1029/2002GL015708.

Cede, A., E. Luccini, L. Nuñez, R. Piacentini, and M. Blumthaler (2002b), Monitoring of erythemal irradiance in the Argentine Ultraviolet Network, *J. Geophys. Res.*, *107*(D13), 4165, doi:10.1029/2001JD001206.

Cereceda, P., P. Osses, H. Larraín, M. Farías, R. Pinto, and R. S. Schemenauer (2002), Advective, orographic and radiation fog in the Tarapacá Region, Chile, *Atmos. Res.*, *64*, 261–271, doi:10.1016/S0169-8095(02)00097-2.

Cereceda, P., H. Larrain, P. Osses, M. Farías, and I. Egaña (2008a), The climate of the coast and fog zone in the Tarapacá Region, Atacama Desert, Chile, *Atmos. Res.*, *87*, 301–311, doi:10.1016/j.atmosres.2007.11.011.

Cereceda, P., H. Larrain, P. Osses, M. Farías, and I. Egaña (2008b), The spatial and temporal variability of fog and its relation to fog oases in the Atacama Desert, Chile, *Atmos. Res.*, *87*, 312–323, doi:10.1016/j.atmosres.2007.11.012.

Charlson, R. J., A. S. Ackerman, F. A.-M. Bender, T. L. Anderson, and Z. Liu (2007), On the climate forcing consequences of the albedo continuum between cloudy and clear air, *Tellus, Ser. B*, *59*, 715–727, doi:10.1111/j.1600-0889.2007.00297.x.

Degünther, M., and R. Meerkötter (1998), Influence of inhomogeneous surface albedo on UV irradiance, paper presented at the European Confer-

ence on Atmospheric UV Radiation, Eur. Comm., Finn. Meterol. Inst., Helsinki, Finland, 28 June–2 July.

Degünther, M., R. Meerkötter, A. Albold, and G. Seckmeyer (1998), Case study on the influence of inhomogeneous surface albedo on UV irradiance, *Geophys. Res. Lett.*, *25*, 3587–3590, doi:10.1029/98GL52785.

Dong, X., T. P. Ackerman, and E. E. Clothiaux (1998), Parameterizations of the microphysical and shortwave radiative properties of boundary layer stratus from ground-based measurements, *J. Geophys. Res.*, *103*, 31,681–31,693, doi:10.1029/1998JD200047.

Dutton, E. G., J. J. Michalsky, T. Stoffel, B. W. Forgan, J. Hickey, D. W. Nelson, T. L. Alberta, and I. Reda (2001), Measurement of broadband diffuse solar irradiance using current commercial instrumentation with a correction for thermal offset errors, *J. Atmos. Oceanic Technol.*, *18*, 297–314, doi:10.1175/1520-0426(2001)018<0297:MOBDSI>2.0.CO;2.

Fitzpatrick, M. F., and S. G. Warren (2005), Transmission of solar radiation by clouds over snow and ice surfaces. Part II: Cloud optical depth and shortwave radiative forcing from pyranometer measurements in the Southern Ocean, *J. Clim.*, *18*, 4637–4648, doi:10.1175/JCLI3562.1.

Fitzpatrick, M. F., R. E. Brandt, and S. G. Warren (2004), Transmission of solar radiation by clouds over snow and ice surfaces: A parameterization in terms of optical depth, solar zenith angle, and surface albedo, *J. Clim.*, *17*, 266–275, doi:10.1175/1520-0442(2004)017<0266:TOSRBC>2.0.CO;2.

Fu, Q., and K. N. Liou (1992), On the correlated *k*-distribution method for radiative transfer in nonhomogenous atmospheres, *J. Atmos. Sci.*, *49*, 2139–2156, doi:10.1175/1520-0469(1992)049<2139:OTCDMF>2.0.CO;2.

Fu, Q., and K. N. Liou (1993), Parameterization of the radiative properties of cirrus clouds, *J. Atmos. Sci.*, *50*, 2008–2025, doi:10.1175/1520-0469(1993)050<2008:POTRPO>2.0.CO;2.

Hartley, A. J., G. Chong, J. Houston, and A. E. Mather (2005), 150 million years of climatic stability: Evidence from the Atacama Desert, northern Chile, *J. Geol. Soc.*, *162*, 421–424, doi:10.1144/0016-764904-071.

Herman, J. R., and E. A. Celarier (1997), Earth surface reflectivity climatology at 340–380 nm from TOMS data, *J. Geophys. Res.*, *102*, 28,003–28,011, doi:10.1029/97JD02074.

Huneeus, N., L. Gallardo, and J. A. Rutllant (2006), Offshore transport episodes of anthropogenic sulfur in northern Chile: Potential impact on the stratocumulus cloud deck, *Geophys. Res. Lett.*, *33*, L19819, doi:10.1029/2006GL026921.

Leontieva, E., and K. Stamnes (1996), Remote sensing of cloud optical properties from ground-based measurements of transmittance: A feasibility study, *J. Appl. Meteorol.*, *35*, 2011–2022, doi:10.1175/1520-0450(1996)035<2011:RSOCOP>2.0.CO;2.

Leszczynski, K., K. Jokela, L. Ylianttila, R. Visuri, and M. Blumthaler (1998), Erythemally weighted radiometers in solar UV monitoring: Results from the WMO/STUK intercomparison, *Photochem. Photobiol.*, *67*, 212–221, doi:10.1111/j.1751-1097.1998.tb05189.x.

Li, Z., and L. Garand (1994), Estimation of surface albedo from space: A parameterization for global application, *J. Geophys. Res.*, *99*, 8335–8350, doi:10.1029/94JD00225.

Loeb, N. G., and J. A. Coakley Jr. (1998), Inference of marine stratus cloud optical depths from satellite measurements: Does 1D theory apply?, *J. Clim.*, *11*, 215–233, doi:10.1175/1520-0442(1998)011<0215:IOMSCO>2.0.CO;2.

Luccini, E., A. Cede, R. Piacentini, C. Villanueva, and P. Canziani (2006), Ultraviolet climatology over Argentina, *J. Geophys. Res.*, *111*, D17312, doi:10.1029/2005JD006580.

McKinlay, A. F., and B. L. Diffey (1987), A reference action spectra for ultraviolet introduced erythema in human skin, in *Human Exposure to Ultraviolet Radiation: Risks and Regulations*, edited by W. R. Passchier and B. M. F. Bosnajakovich, pp. 83–87, Elsevier, New York.

Mims, F. M., and J. E. Frederick (1994), Cumulus clouds and UV-B, *Nature*, *371*, 291, doi:10.1038/371291a0.

Minnis, P., and E. Harrison (1984), Diurnal variability of regional cloud and clear-sky radiative parameters derived from GOES data. Part III: November 1978 Radiative Parameters, *J. Clim. Appl. Meteorol.*, *23*, 1032–1051, doi:10.1175/1520-0450(1984)023<1032:DVORCA>2.0.CO;2.

Otero, L., P. Ristori, B. Holben, and E. Quel (2006), Aerosol optical thickness at ten AERONET-NASA stations during 2002, *Opt. Pura Apl.*, *39*, 355–364.

Rivas, M., E. Luccini, E. Rojas, and R. Piacentini (2000), Irradiancia eritémica y riesgo solar en Arica, norte de Chile, *Energ. Renovables Medio Ambiente*, *8*, 13–16.

Rivas, M., E. Rojas, R. Piacentini, and E. Luccini (2008), UV Index characterization at Arica, north of Chile: Actions to prevent damage to the human health in the region, paper presented at IV Latin American Congress of Photobiology and Photomedicine, Lat. Am. Soc. of Photobiol. and Photomed., Porto Alegre, Brazil, 16–18 Oct.

Rose, F. G., and T. P. Charlock (2002), New Fu-Liou code tested with ARM Raman Lidar and CERES in pre-CALIPSO exercise, paper presented at the 11th Conference on Atmospheric Radiation, Am. Meteorol. Soc., Ogden, Utah.

Schemenauer, R. S., H. Fuenzalida, and P. Cereceda (1988), A neglected water resource: The camanchaca of South America, *Bull. Am. Meteorol. Soc.*, *69*, 138–147, doi:10.1175/1520-0477(1988)069<0138:ANWRTC>2.0.CO;2.

Tsvetsinskaya, E. A., C. B. Schaaf, F. Gao, A. H. Strahler, and R. E. Dickinson (2006), Spatial and temporal variability in Moderate Resolution Imaging Spectroradiometer–derived surface albedo over global arid regions, *J. Geophys. Res.*, *111*, D20106, doi:10.1029/2005JD006772.

Wood, R., et al. (2006), VOCALS-Southeast Pacific Regional Experiment (REx): Scientific program overview, 34 pp., Natl. Cent. for Atmos. Res., Earth Obs. Lab., Boulder, Colo. [Available at http://www.eol.ucar.edu/projects/vocals/science_planning/VOCALS_SPO_rev_aug06.pdf.]

P. Canziani, Equipo Interdisciplinario Para el Estudio de Procesos Atmosféricos en el Cambio Global, Pontificia Universidad Católica Argentina, Alicia Moreau de Justo 1600, Buenos Aires C1107AFF, Argentina.

E. Luccini, Grupo de Energía Solar, Instituto de Física de Rosario, Consejo Nacional de Investigaciones Científicas y Técnicas, Bv. 27 de Febrero 210bis, CP 2000, Rosario, Argentina. (luccini@ifir-conicet.gov.ar)

M. Rivas and E. Rojas, Laboratorio de Radiación Solar Ultravioleta, Departamento de Física, Facultad de Ciencias, Universidad de Tarapacá, Casilla 7-D, Arica, Chile.